THE STUDY ON THE SPACE CHARGE EFFECTS OF RCS/CSNS

S. Xu, S. Fang, S. Wang,* Institute of High Energy Physics (IHEP), Beijing, 100049, China

Abstract

The China Spallation Neutron Source (CSNS) is an accelerator-based facility. It operates at a 25 Hz repetition rate with an initial design beam power of 100 kW and is upgradeable to 500 kW. The accelerator of CSNS consists of a low energy linac and a Rapid Cycling Synchrotron (RCS). The RCS is a key component of CSNS. In this kind of high intensity RCS, the beam is space charge dominated, and the space charge effects are the main source of beam loss. Many simulation works were done for the study of space charge effects for CSNS/RCS by using the codes ORBIT and SIMPSONS. Various conditions are considered in the simulations, including the effects of different lattice structure, different tunes, the combine effect of sextupole field and space charge, different painting beam distribution, etc. The beam loss and emittance growth are compared for different conditions.

INTRODUCTION

The China Spallation Neutron Source (CSNS) is based on a high power accelerator, which consists of a 80 MeV linac, a 1.6 GeV rapid cycling synchrotron and beam transport lines [1]. The accelerator complex is designed to deliver a beam power of 100 kW at a 25 Hz repetition rate, with an upgrade capability of up to 500 kW by raising the linac output energy and increasing the intensity. The RCS is a key component of CSNS. It accumulates a beam injected at 80 MeV, accelerates the beam to a design energy of 1.6 GeV, and extracts the high energy beam to the target. Due to the high beam density and high repetition rate, the rate of beam loss must be controlled to a very low level. In this kind of high power RCS, especially at the low energy end, the beam is space charge dominated, and the space charge effects are the main source of beam loss. The space charge effects limit the maximum beam density, as well as beam power. Many simulations were done to study space charge effects in CSNS/RCS by using the codes ORBIT and SIMPSONS. Various conditions, which may influence the space charge effects and beam loss, are considered, including the effects of different lattice structure, different tune, the combine effect of sextupole field and space charge, different painting beam distribution, etc. The beam loss and emittance growth are compared for different conditions. The simulation results are the foundation of physics design and the choice of design parameters. To control the uncontrolled beam loss, the transverse and momentum beam collimation systems are designed. With the beam collimation, the uncontrolled beam loss can be compressed to less than 1W/m.

* wangs@ihep.ac.cn

The present lattice of the CSNS/RCS is a triplet based fourfold structure, as shown in Fig. 1. Table 1 shows the main parameters of the lattice.

Table 1: Main Parameters of the Lattice

Circumference (m)	228
Superperiod	4
Number of dipoles	24
Number of long drift	12
Total Length of long drift (m)	75
Betatron tunes (h/v)	4.82/4.80
Chromaticity (h/v)	-4.3/-8.2
Momentum compaction	0.041
RF harmonics	2
RF Freq. (MHz)	1.0241~2.3723
Trans. acceptance (μπm.rad)	540
RF Voltage (kV)	165

SPACE CHARGE EFFECTS DURING INJECTION

Painting Schemes

Two painting schemes—correlated and anti-correlated painting—are both available in the injection of CSNS/RCS. For correlated painting, both the emittance ε_x and ε_y are painted from small to large during injection. It produces a rectangular transverse beam profile without space charge effects. For anti-correlated painting, the emittance is painted from small to large in one direction, and from large to small in the other direction (vertical direction here). It produces an elliptical transverse beam profile without space charge effects. In the case of disregarding space charge effects, the painting beam density is uniform. Figs. 2 and 3 show simulation results of painting with and without space charge effects. The upper left and right graphs show the particles distribution in (x, x') and (y, y') phase space respectively. The lower graphs show the distribution in (x, y) space and the emittance evolution during painting.

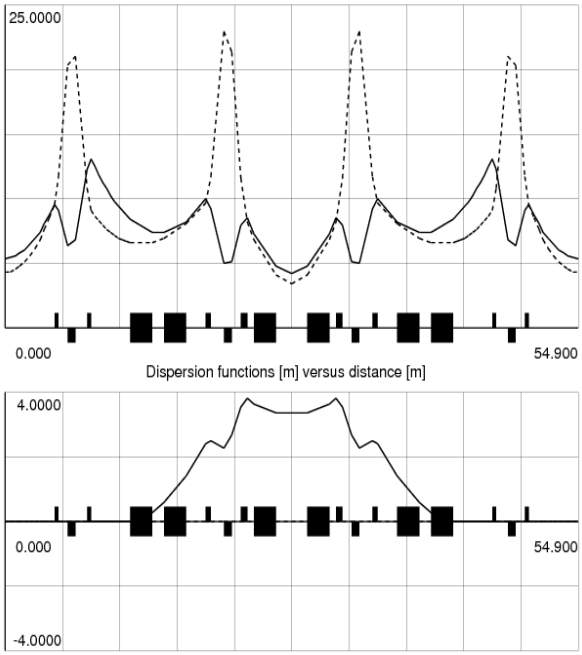

Fig. 1: Twiss parameters of one superperiod.

As shown in Fig. 2 (a) and Fig. 3 (a), the results of painting without space charge effects are just as predicted. Due to space charge effects, some halo particles are generated, and beam emittance is increased somehow.

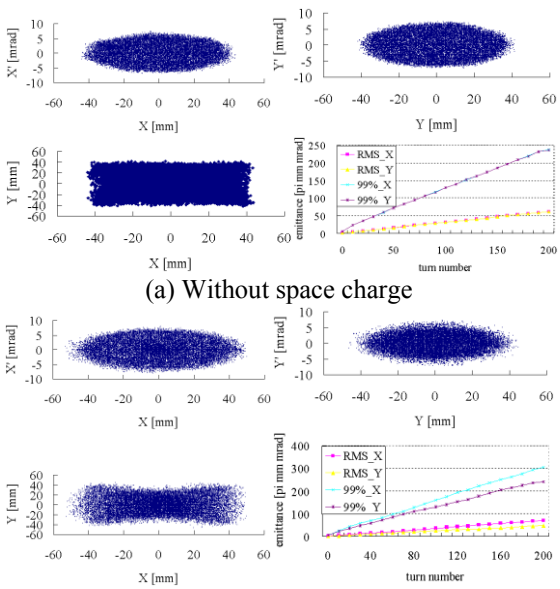

(a) Without space charge

(b) With space charge

Fig. 2: Particles distributions and emittance evolution from correlated painting without (a) and with (b) space charge effects.

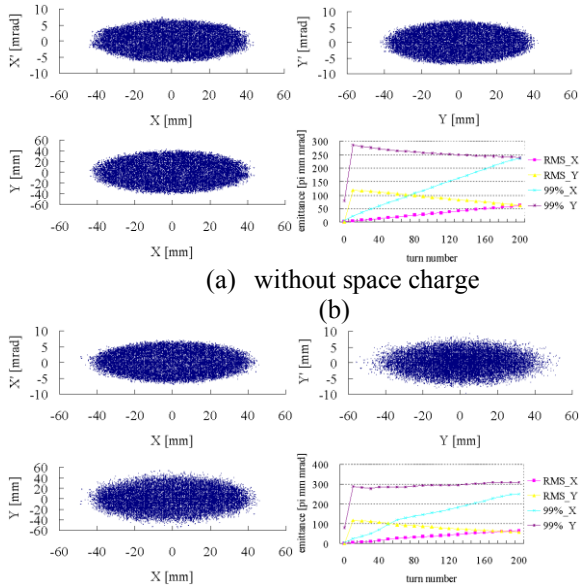

(a) without space charge

(b) including space charge

Fig. 3: Particles distributions and emittance evolution from anti-correlated painting without (a) and with (b) space charge effects.

Fig. 4 shows Poincaré maps of one test particle during different injection time-periods by correlated painting, in which the filamentation is observed. For anti-correlated painting, since both x and y emittance are painted from small to large during injection, the beam profile is susceptible to transverse coupling. However it has the capability of painting over the halo, while in the case of anti-correlated painting, it is immune to the transverse coupling, but it does not have the capability of painting over the halo in one direction (vertical shown here) [2].

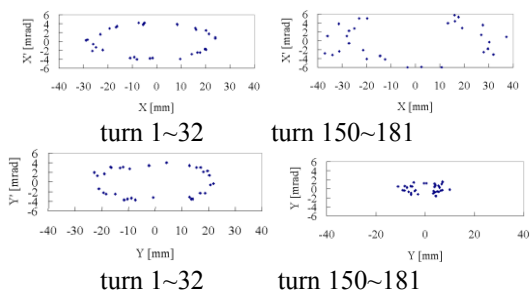

Fig. 4: Poincaré maps of one test particle during different injection time-periods from correlated painting.

Injection Painting Optimization

In order to reduce the transverse space charge effects, it is essential to produce a uniform longitudinal distribution. As shown in Figure 5, obtained by using ORBIT, much uniform longitudinal distribution can be obtained by using momentum offset in the injection painting procedure.

To investigate the diffusion motion of particles, all the particles are divided into three parts in (y, y') phase

space, outer part, middle part and inner region, as shown in Fig. 6, indicated by different colours. Due to space charge effects, Diffusion occurs among different parts, as shown in Figure 6(a). The diffusion results in the change of beam distribution, and the generation of halo particles. In order to produce much uniform transverse distribution and reduce halo production, two ways were tried to optimize the painting orbit bumps: painting a smaller emittance than the target value (case 1), injecting less particles in the inner and outer region of the emittance space (case 2). However, for case 1, this way results in small RMS emittance and large tune shift, which may be troublesome in the presence of magnet errors [3]. Fig. 7 and Fig. 8 show beam distributions and tune spreads of test particles with different injection painting respectively. The beam distribution in case 1 has a peak top, and large tune spread. The beam distribution of case 2 with a relatively flat beam density is more uniform.

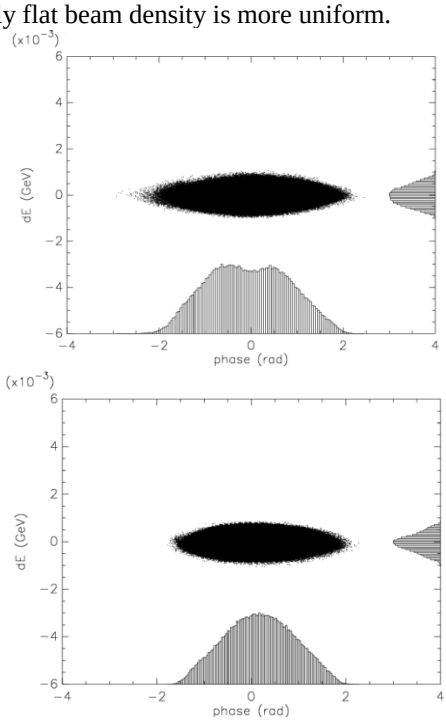

Fig. 5: Particle distributions in (φ, ΔE) phase space after painting with (top) and without (bottom) momentum offset.

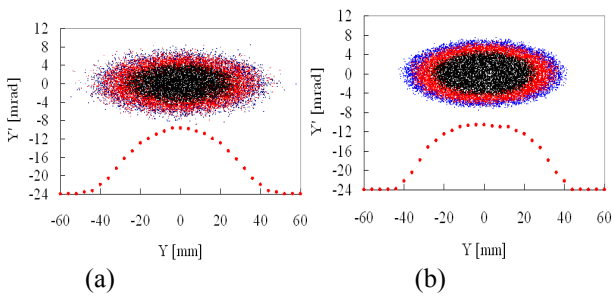

Fig. 6: Particles distribution in (y, y') phase space after painting with (a) and without (b) SC from the anti-correlated painting.

SPACE CHARGE EFFECTS DURING RAMPING

The initial beam distribution is produced by anti-correlated painting with a momentum offset. Fig. 9 shows the time evolution of the 99% unnormalized emittance in early-stage ramping. The unnormalized emittance should be depressed with $1/\beta\gamma^2$ without space charge effects. Due to space charge effects, there is apparent emittance growth in horizontal direction at the beginning of ramping. The study is focused on this time-period.

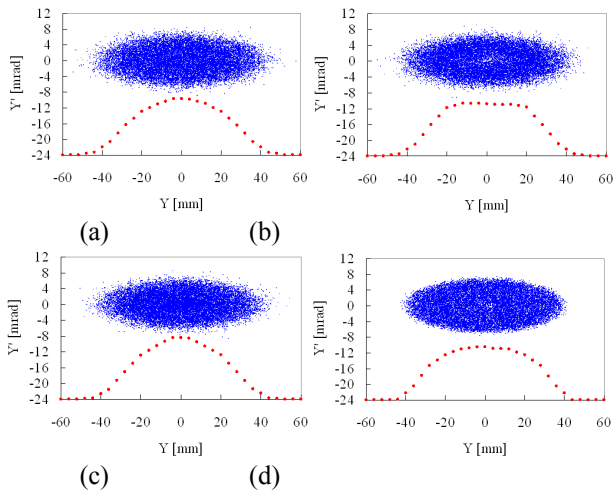

Fig. 7: Beam distributions in (y, y') phase space after painting by different injection orbit bumps: (a) uniform painting; (b) injecting less particles in the inner and outer region of the emittance space; (c) painting a smaller emittance than the target value; (d) uniform painting without SC.

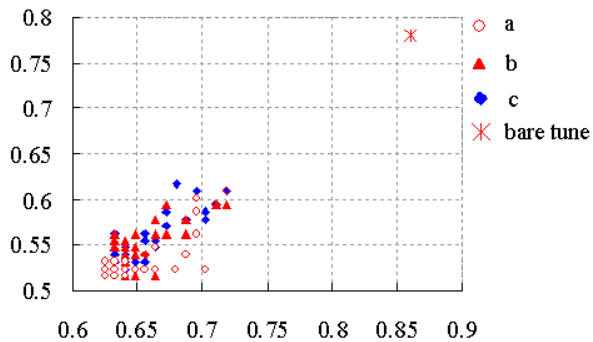

Fig. 8: Tune spreads of test particles with different painting distributions: (a) injecting particles a smaller emittance than the target value; (b) injecting less particles in the inner and outer region of the emittance space; (c) uniform painting.

Fig. 10 shows diffusion of particles among different parts during ramping. The red dots indicate the distribution just after the painting (200 turns). The blue dots indicate the distribution after 400 turns. Some particles move towards the inner region of the phase

space during ramping, while some towards the outer region. The diffusion among three parts is clearly observed.

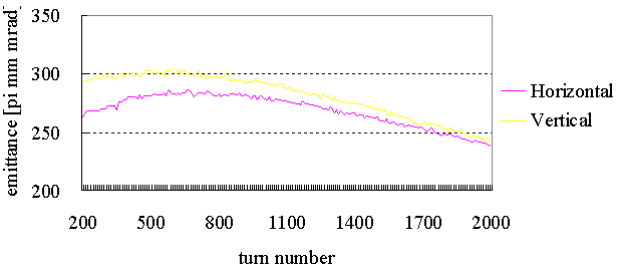

Fig. 9: Time evolution of the 99% emittance.

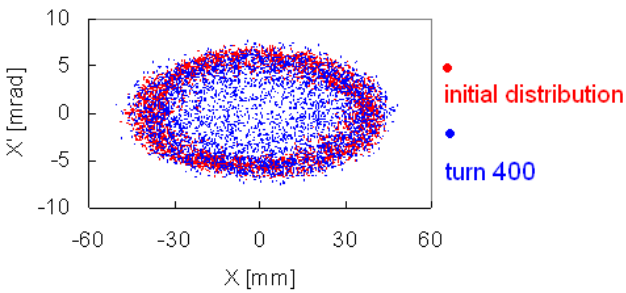

(a) particles in the outer region

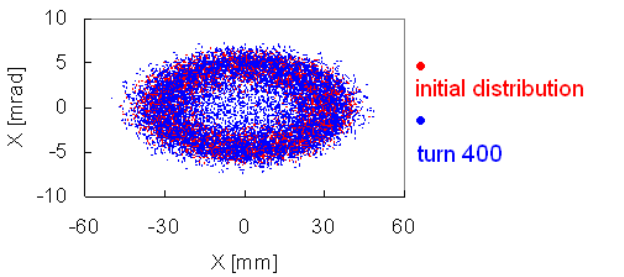

(b) particles in the middle region

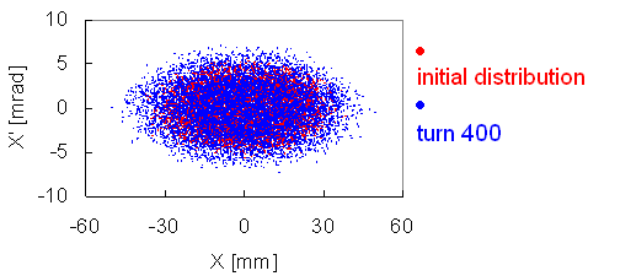

(c) particles in the inner region

Fig. 10: Diffusion of particles among different parts during ramping.

Since the simulation does not include magnet errors, the emittance growth and particle distribution change must be driven by the beam itself (space charge force). There are several possible driving mechanisms such as (1) pure evolution of any coherent mode not related to resonance of an individual particle; (2) pure nonlinear resonance originating from the space charge; (3) coupling resonance with the coherent modes [4]. More work will be done to study the mechanism here.

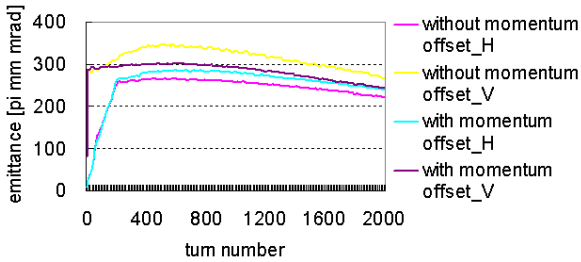

Fig. 11: Time evolution of the 99% emittance with and without momentum offset during injection.

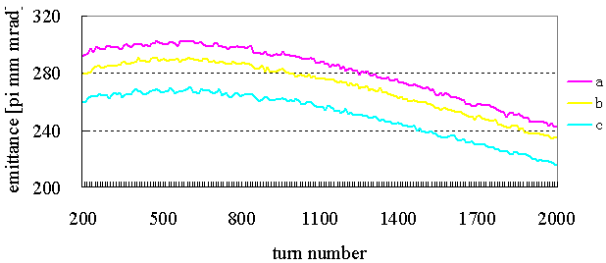

Fig. 12: Time evolution of the vertical 99% emittance with different initial distributions. Lines (a) (b) (c) indicate using the particles distribution of (a) (b) (c) in Fig. 7 as the initial distributions, respectively.

Simulations were also made to study emittance growth due to different painted distributions. The effects of different longitudinal distribution are first investigated. As described in Figs. 5 and 11, with a momentum offset during the injection painting, the longitudinal distribution after painting is much uniform and the emittance growth during ramping is less. Fig. 12 shows the time evolution of the vertical 99% emittance during ramping for different initial distributions. All the initial distributions are produced by anti-correlated painting (by 200 turns) with a momentum offset, but with different injection orbit bumps. All the initial transverse distributions show a similar trend of emittance growth without magnet errors.

EMITTANCE GROWTH VS. TUNES

The dependence of emittance growth on tunes was considered. Tunes around design values of 4.82/4.80 and with a split of 0.5 were compared. In simulations, anti-correlated painting scheme without momentum offset was adopted. Further work will be done to study the tune effects in the case of using momentum offset in the injection painting procedure. Fig. 13 plots the maximum 99% emittance during ramping vs. the bare horizontal tune, where the vertical tune was fixed to 4.78. Fig. 14 presents the time evolution of the 99% emittance with different bare tunes. There is less emittance growth at the tune of just below the integer tune. For the tune 4.82/4.36, there is large emittance growth. Fig. 15 shows the Poincaré maps of two test particles during ramping with

the bare tune 4.82/4.36, in which particles are trapped by the structure resonance Q_y=4. Because the magnet errors are not included in the simulations, the structure resonance is excited by space charge force [5]. It is apparent that the choice of tune is very important.

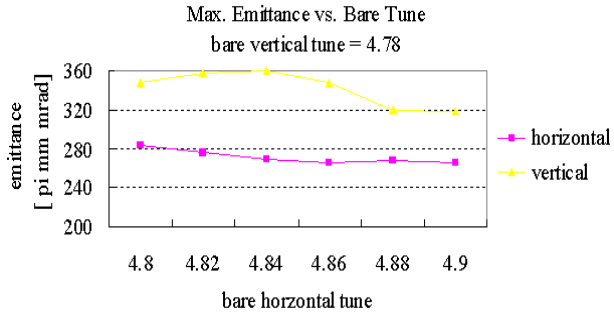

Fig. 13: Maximum 99% emittance during ramping vs. the bare horizontal tune.

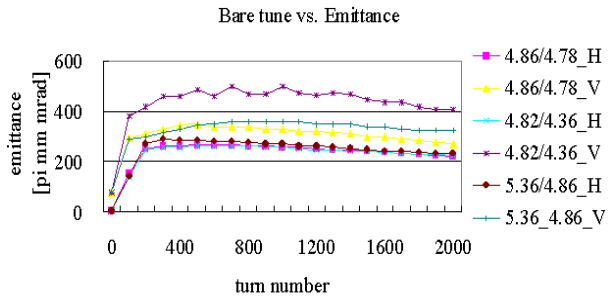

Fig. 14: Time evolution of 99% emittance with different bare tunes.

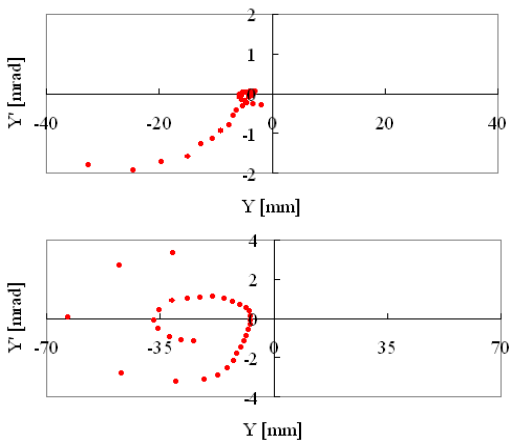

Fig. 15: Poincaré maps of two test particles during ramping with the bare tune 4.82/4.36.

DEPENDENCE ON LATTICE TYPE

To investigate the dependence of emittance growth on the lattice type, another two lattices, named as Lattice-B and Lattice-C, were introduced in simulation for compare. As shown in table 2, the lattice B consists of FODO cells in the arcs and doublet in the dispersion free straight sections, while Lattice-C consists of full FODO structure. In this section anti-correlated painting scheme without momentum offset were still adopted. Fig.16 shows the time evolution of the 99% emittance for different lattice types. Lattice-C looks better in the point of view of emittance growth.

SUMMARY

Space charge effects have been studied by simulations, including the space charge effects in painting, ramping, and the dependence of space charge effects on the bare tune and lattice type. Some injection painting optimizations were made for decreasing halo formation and tune spread. The choice of bare tune is very important. The choice of lattice structure also influences the emittance growth. All the simulations in this paper do not include the magnet field errors. Further work will involve the combine effects of space charge effects magnet field errors.

ACKNOWLEDGMENT

The authors would like to thank Shinji Machida for providing the SIMPSONS code and help on the test run.

Table 2: Parameters of lattices

	Lattice-B	Lattice-C
Structure	FODO+ Doublet	FODO
Circumference (m)	248	239.6
Super-periods	4	4
Qx/Qy	5.86/5.78	5.86/5.78
Max. straight (m)	9.3	4.5

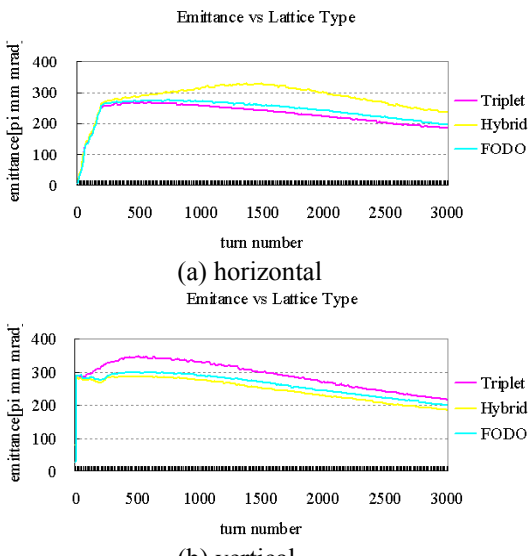

Fig. 16: Time evolution of the (a) horizontal and (b) vertical 99% emittance.

REFERENCES

[1] CSNS Feasibility Study Report, June, 2009, IHEP.
[2] J. Beebe-Wang *et al,* "Space Charge and Magnet Error Simulation for the SNS Accumulator Ring", p. 1286, Proc. of EPAC2000.
[3] J. Galambos *et al,* "SNS Injection Simulations with Space Charge", p. 3140, Proc. of PAC99.
[4] Accelerator Technical Design Report for High-Intensity Proton Accelerator Facility Project, J-PARC.
[5] S. Machida, "Space Charge Effects in Low-Energy Proton Synchrotrons", Nucl. Instr. & Meth. A309, (1991) 43-59.